Increased circulating sclerostin levels in end-stage renal disease predict biopsy-verified vascular medial calcification and coronary artery calcification

Abdul Rashid Qureshi[1,6], Hannes Olauson[1,6], Anna Witasp[1], Mathias Haarhaus[1], Vincent Brandenburg[2], Annika Wernerson[1], Bengt Lindholm[1], Magnus Söderberg[3], Lars Wennberg[4], Louise Nordfors[1], Jonaz Ripsweden[5], Peter Barany[1] and Peter Stenvinkel[1]

[1]Division of Renal Medicine and Baxter Novum, Department of Clinical Sciences, Intervention and Technology, Karolinska Institutet, Stockholm, Sweden; [2]Department of Cardiology, University Hospital RWTH Aachen, Aachen, Germany; [3]Pathology, Drug Safety and Metabolism, AstraZeneca, Mölndal, Sweden; [4]Division of Transplantation Surgery, Department of Clinical Sciences, Intervention and Technology, Karolinska Institutet, Stockholm, Sweden and [5]Division of Radiology, Department of Clinical Sciences, Intervention and Technology, Karolinska Institutet, Stockholm, Sweden

Sclerostin, an osteocyte-derived inhibitor of bone formation, is linked to mineral bone disorder. In order to validate its potential as a predictor of vascular calcification, we explored associations of circulating sclerostin with measures of calcification in 89 epigastric artery biopsies from patients with end-stage renal disease. Significantly higher sclerostin levels were found in the serum of patients with epigastric and coronary artery calcification (calcification score 100 or more). In Spearman's rank correlations, sclerostin levels significantly associated with age, intact parathyroid hormone, bone-specific alkaline phosphatase, and percent calcification. Multivariable regression showed that age, male gender, and sclerostin each significantly associated with the presence of medial vascular calcification. Receiver operating characteristic curve analysis showed that sclerostin (AUC 0.68) predicted vascular calcification. Vascular sclerostin mRNA and protein expressions were low or absent, and did not differ between calcified and non-calcified vessels, suggesting that the vasculature is not a major contributor to circulating levels. Thus, high serum sclerostin levels associate with the extent of vascular calcification as evaluated both by coronary artery CT and scoring of epigastric artery calcification. Among circulating biomarkers of mineral bone disorder, only sclerostin predicted vascular calcification.

Kidney International advance online publication, 2 September 2015; doi:10.1038/ki.2015.194

KEYWORDS: end-stage renal disease; inflammation; mineral-bone disease; sclerostin; vascular calcification

Correspondence: *Peter Stenvinkel, Division of Renal Medicine M99, Karolinska University Hospital at Huddinge, Stockholm 141 86, Sweden. E-mail: peter.stenvinkel@ki.se*

[6]The first two authors contributed equally to this work.

Received 20 January 2015; revised 18 May 2015; accepted 21 May 2015

Vascular calcification and bone disorders are features of the uremic phenotype entitled chronic kidney disease-mineral and bone disorder (CKD-MBD),[1] which begins early in the course of CKD and contributes to increased morbidity and mortality in this prematurely aged patient population.[2,3] Smoldering alterations in mineral homeostasis during worsening of kidney function promote vascular calcification, cardiovascular disease (CVD), bone disease, and poor outcome.[4] The mechanisms causing the CKD-MBD syndrome are not yet fully elucidated, but seem in part to be associated with the stimulation of osteocyte secretion. Although several biomarkers of CKD-MBD, such as calcium, phosphate, parathyroid hormone (iPTH),[5] fibroblast growth factor-23 (FGF23),[6] and bone-specific alkaline phosphatase (bALP)[7] predict outcome in end-stage renal disease (ESRD), there is a need of a biomarker that could predict the presence and extent of vascular calcification as well as outcome.

Among several emerging factors implicated in CKD-MBD, sclerostin, a osteocyte-derived glycoprotein has attracted recent interest.[8] Sclerostin acts as a soluble inhibitor of the Wnt signaling pathway and its physiological role is to reduce bone formation. The serum sclerostin levels increase with the progression of CKD[8,9] even though the renal elimination of sclerostin is reported to increase when renal function deteriorates,[10] whereas the levels decrease rapidly after renal transplantation (RTx).[11] These changes are likely explained by changes in the production of sclerostin in the bone,[12] and possibly other tissues, as renal function changes. This was supported by Fang *et al.*[13] who reported that increased osteocytic protein secretion, vascular calcification, and stimulated vascular osteoblastic transition occur already in early CKD. Although sclerostin is a soluble inhibitor of osteoblast function, positive correlations of serum sclerostin with bone mineral density have been reported in patients with Type 2 diabetes[14] and CKD patients.[15,16]

Mutations in the *SOST* gene, coding for sclerostin, associate with enhanced Wnt signaling, and lead to a phenotype characterized by marked increases in bone mineral density, bone volume, and bone formation.[17] Sclerostin antibodies are currently being evaluated in clinical trials as a treatment option for osteoporosis in postmenopausal women.[18] However, as sclerostin may also have extraskeletal effects,[19] the potential role of sclerostin in extraosseous calcification, in particular vascular calcification, needs to be further explored. Whereas circulating sclerostin was inversely related to the presence of calcified carotid artery plaques in patients with Type 2 diabetes,[14] a study in hemodialysis patients showed a positive correlation between sclerostin and the amount of aortic valve calcification.[20] On the other hand, a negative correlation was found between sclerostin and signs of vascular calcifications (Kauppila method) in a multivariate model including 164 hemodialysis patients.[21] Claes *et al.*[22] reported that the positive univariate correlation between aortic calcifications and sclerostin levels in predialysis patients became inverse in a multivariate model. Based on the effects by sclerostin on bone, one may speculate that increased levels of sclerostin counterregulate the progression of vascular calcification by inhibiting the mineralization process also in the vasculature. On the other hand, Fang *et al.*[8] recently showed that neutralization by a monoclonal antibody against the Dickkopf-related protein 1, which was similar to sclerostin is a Wnt inhibitor secreted mainly by osteocytes, leads to decreased levels of sclerostin, corrected osteodystrophy, and prevented CKD–induced vascular calcification in diabetic mice. However, in contrast to Dickkopf-related protein 1, sclerostin effects are tissue and context dependent even at times capable of stimulating Wnt signaling. As circulating Wnt inhibitors are involved in the pathogenesis of CKD-MBD, and as sclerostin serves as a regulator of the mineralization process in bone and potentially also in the vasculature, it could be hypothesized that elevated sclerostin levels predict poor outcome.

To date, clinical data on sclerostin as an outcome biomarker are inconsistent and elevated sclerostin have been reported to predict either higher mortality,[9,23] lower mortality,[24,25] or not being related to outcome.[21] These contradictory results imply that confounders need to be identified and accounted for. In the current study, we measured circulating sclerostin and other CKD-MBD biomarkers, inflammation biomarkers, body composition, and degree of coronary artery calcification (CAC) score by cardiac computed tomography (CT) in ESRD patients undergoing living donor RTx. Furthermore, the presence and extent of vascular calcification and protein mRNA expression of sclerostin in calcified and non-calcified vasculature were ascertained in vascular biopsies from the inferior epigastric artery. The extensive phenotyping allowed us to explore and validate the predictive role of the presence of vascular calcification with CAC score and several CKD-MBD biomarkers.

RESULTS

Demographics and clinical characteristics of the ESRD patients undergoing living donor RTx are shown in Table 1. Median S-creatinine did not differ significantly in dialyzed (784 μmol/l) versus non-dialyzed (664 μmol/l) patients. Similarly, median sclerostin level did not differ significantly in dialyzed (468 pg/ml) versus non-dialyzed (414 pg/ml) patients. Higher circulating sclerostin levels were found in patients with histological signs of moderate–extensive vascular calcification ($P=0.003$) (Figure 1). Nineteen patients with CAC score $\geqslant 100$ Agatston units (AU) by cardiac CT had significantly higher median levels of sclerostin compared with 46 patients with CAC score <100 AU (559 vs. 367 pg/ml; $P=0.001$) (Figure 1). No significant difference ($P=0.22$) in median sclerostin levels was found between diabetic (563 pg/ml) and non-diabetic (432 pg/ml) patients. In Spearman's rank (ρ) correlations, sclerostin concentrations were significantly associated with age ($\rho=0.38$; $P=0.002$), iPTH ($\rho=-0.33$; $P=0.002$), S-creatinine ($\rho=0.26$; $P=0.015$), high-density lipoprotein-cholesterol (HDL-cholesterol) ($\rho=-0.23$; $P=0.03$), lipoprotein(a) ($n=84$; $\rho=0.29$; $P=0.008$), skin advanced glycation end-product autofluorescence ($n=66$; $\rho=0.32$; $P=0.009$), calcium ($\rho=0.26$; $P=0.02$), bALP ($n=83$; $\rho=-0.37$; $P=0.0006$), total osteocalcin ($\rho=-0.24$; $P=0.03$), inactive (GLU) undercarboxylated osteocalcin ($\rho=-0.23$; $P=0.04$) and active (GLA) carboxylated osteocalcin ($\rho=-0.28$; $P=0.01$), tumor necrosis factor (TNF) ($\rho=0.24$; $P=0.03$), and 8-hydroxy-2′-deoxyguanosine ($\rho=0.23$; $P=0.04$). Sclerostin levels were not associated with gender, high-sensitivity C-reactive protein (hsCRP), interleukin-6, bone mineral density, phosphate, magnesium, troponin-T, 25(OH)D-vitamin, 1,25(OH)D-vitamin, cholesterol, triglycerides, pentosidine, or klotho. A multivariate regression model for determinants for plasma sclerostin showed that age ($\beta=0.41$; $P=0.007$), S-creatinine ($\beta=0.30$; $P=0.01$), and iPTH ($\beta=-0.25$; $P=0.05$) were associated with plasma sclerostin levels (Table 2). Eleven patients with pre-existing CVD had significantly higher median total CAC score (970 (0–3816) vs. 0 (0–455) AU; $P=0.001$) compared with 54 non-CVD patients.

Determinants of vascular calcification

Scoring by the pathologist. Moderate and extensive vascular calcification was present in 37 (42%) of 89 patients. As expected (Table 1), ESRD patients with vascular calcification were older ($P<0.001$), more often males ($P=0.04$), diabetics ($P=0.003$), and had higher body mass index ($P=0.002$). Moreover, patients with vascular calcification had significantly higher median total CAC score (133 vs. 0 AU; $P<0.001$), troponin T (23.5 vs. 14.0 μg/l; $P=0.04$), TNF (11.8 vs. 10.0 pg/ml; $P=0.03$), and lower median insulin growth factor-1 (IGF-1) (189 vs. 264 ng/ml; $P=0.03$) and HDL-cholesterol (1.2 vs. 1.5 mmol/l; $P=0.04$) levels. The association between magnitude of vascular calcification and total CAC scores by CT of the heart is depicted in Figure 2. In univariate analysis, sclerostin levels were significantly higher

in patients with vascular calcification (523 vs. 367 pg/ml; $P = 0.003$). Total bone mineral density was not statistically different among ESRD patients with and without vascular calcification. A multivariable GENMOD regression (risk ratio (RR), 95% confidence inter al (CI)) analysis (including age, gender, and sclerostin) showed that age (2.12 (1.23–3.62);

Table 1 | Demographic and biochemical characteristics of end-stage renal disease patients

	All patients ($n = 89$)	Group 1: No-minimal vascular calcification ($n = 52$)	Group 2: Moderate–extensive vascular calcification ($n = 37$)	*P*-values group 1 versus 2
Demography and metabolic biomarkers				
Age (years)	46 (24–62)	40 (22–60)	53 (37–66)	**<0.001**
Males (%)	63	54	76	**0.04**
Diabetes mellitus (%)	18	8	32	**0.003**
Cardiovascular disease (%)	19	6	38	**<0.001**
Dialysis vintage (years)	0.3 (0–3.1)	0.3 (0–1.6)	0.7 (0–3.9)	0.09
Body mass index (kg/m^2)	24.1 (19.8–27.9)	23.1 (19.8–26.4)	24.7 (21.9–29.4)	**0.002**
Total fat mass (kg)[a,b]	20.8 (6.6–31.4)	15.1 (5.7–31.8)	23.9 (8.9–32.8)	0.10
Systolic blood pressure (mm Hg)	139 (115–166)	136 (114–165)	144 (113–169)	0.16
Diastolic blood pressure (mm Hg)	85 (65–97)	85 (64–97)	82 (65–100)	0.50
Hemoglobin (g/l)	114 (97–135)	114 (96–135)	115 (99–137)	0.73
Insulin growth factor-1 (ng/ml)	258 (131–381)	264 (146–391)	189 (115–364)	**0.03**
Triglycerides (mmol/l)	1.3 (0.7–2.6)	1.2 (0.7–2.5)	1.6 (0.8–2.8)	0.10
Cholesterol (mmol/l)	4.6 (3.3–6.3)	4.7 (3.6–5.7)	4.4 (3.0–6.7)	0.33
HDL-cholesterol (mmol/l)	1.4 (0.8–2.0)	1.5 (1.0–1.9)	1.2 (0.8–2.1)	**0.04**
Lipoprotein (a) (mg/l)[c]	155 (50–933)	177 (50–777)	149 (50–1122)	0.80
Creatinine (μmol/l)	740 (500–1086)	710 (482–1120)	775 (498–1030)	0.77
Troponin-T (μg/l)	17.0 (0.02–53.8)	14.0 (0.01–45.8)	23.5 (0.05–63.3)	**0.04**
Vascular calcification and mineral-bone disease biomarkers				
Vascular calcification (%)[d]	1.7 (0.1–25.2)	0.8 (0.1–2.0)	9.3 (2.9–41.4)	**<0.001**
Bone mineral density (g/cm^2)[a,b]	0.91 (0.68–1.07)	0.89 (0.72–1.08)	0.92 (0.56–1.02)	0.55
Cardiac CT (Agatston units)[e]	3 (0–1666)	0 (0–271)	133 (0–2871)	**<0.001**
Sclerostin (pg/ml)	440 (230–857)	367 (203–847)	523 (357–1012)	**0.003**
Intact parathyroid hormone (ng/l)	252 (80–637)	240 (97–704)	334 (823–816)	0.35
Calcium (mmol/l)	2.3 (2.1–2.5)	2.3 (2.1–2.6)	2.3 (2.0–2.5)	0.65
Phosphate (mmol/l)	1.6 (1.0–2.3)	1.7 (1.0–2.3)	1.6 (1.0–2.4)	0.59
Magnesium (mmol/l)	0.9 (0.7–1.1)	0.8 (0.7–1.0)	0.9 (0.7–1.1)	0.65
Total osteocalcin (ng/ml)	70.2 (16.8–298.7)	62.5 (23.5–300.5)	70.8 (11.5–281.7)	0.51
GLU osteocalcin (ng/ml)	15.8 (2.1–93.4)	15.9 (2.8–96.2)	13.4 (1.5–96.7)	0.29
GLA osteocalcin (ng/ml)	32.5 (11.6–103.6)	34.0 (12.0–91.5)	31.8 (10.3–116.2)	0.83
25(OH) D-vitamin (nmol/l)	37 (20–67)	36 (18–63)	37 (21–95)	0.43
1,25(OH) D-vitamin (ng/l)	17 (9–34)	17 (10–30)	19 (7–40)	0.39
FGF-23 (pg/ml)	4055 (711–53187)	3839 (447–39187)	5279 (817–89120)	0.58
Alkaline phosphatase (U/l)	60.6 (38.2–122.6)	58.9 (37.7–138.5)	64.5 (39.7–90.9)	0.83
Bone alkaline phosphatase (μg/l)[f]	15.8 (9.2–43.9)	15.7 (10.0–57.4)	16.2 (9.0–32.1)	0.27
Fetuin A (g/l)	0.24 (0.15–0.30)	0.24 (0.17–0.30)	0.23 (0.14–0.28)	0.10
Klotho (pg/ml)	363 (190–601)	363 (181–662)	342 (198–564)	0.94
Inflammation biomarkers				
C-reactive protein (mmol/l)	1.0 (0.2–9.0)	0.7 (0.2–7.6)	1.0 (0.2–9.8)	0.17
Albumin (g/l)	36 (32–41)	36 (32–42)	36 (32–41)	0.82
Tumor necrosis factor (pg/ml)	10.5 (7.6–16.8)	10.0 (7.3–15.9)	11.8 (7.9–18.0)	**0.04**
Pentraxin-3 (ng/ml)	4.2 (0.6–9.2)	3.8 (0.6–10.5)	4.8 (1.3–7.9)	0.25
Interleukin-6 (pg/ml)	0.9 (0.01–3.6)	0.9 (0.01–3.1)	1.1 (0.01–7.2)	0.51
Oxidative stress and AGE biomarkers				
Pentosidine (nmol/l)	776 (398–1698)	744 (369–1813)	815 (486–1615)	0.68
AGE, skin autofluorescence[g]	3.1 (2.2–4.1)	3.0 (2.0–4.0)	3.2 (2.5–4.2)	0.11
8-OHdG (ng/ml)	0.18 (0.08–0.38)	0.17 (0.09–0.35)	0.20 (0.08–0.43)	0.40

Abbreviations: AGE, advanced glycation end products; CT, computed tomography; DXA, dual-energy X-ray absorptiometry; FGF, fibroblast growth factor; GLA, carboxylated active form; GLU, undercarboxylated inactive form; HDL, high-density cholesterol; 8-OHdG, 8-hydroxy-2'-deoxyguanosine.
Data are presented as median (range 10th–90th percentile) or percentage. Significant data in bold.
[a]$N = 42$.
[b]By DXA.
[c]$N = 84$.
[d]By semiautomated quantification ($n = 86$).
[e]$N = 65$.
[f]$N = 83$.
[g]$N = 66$.

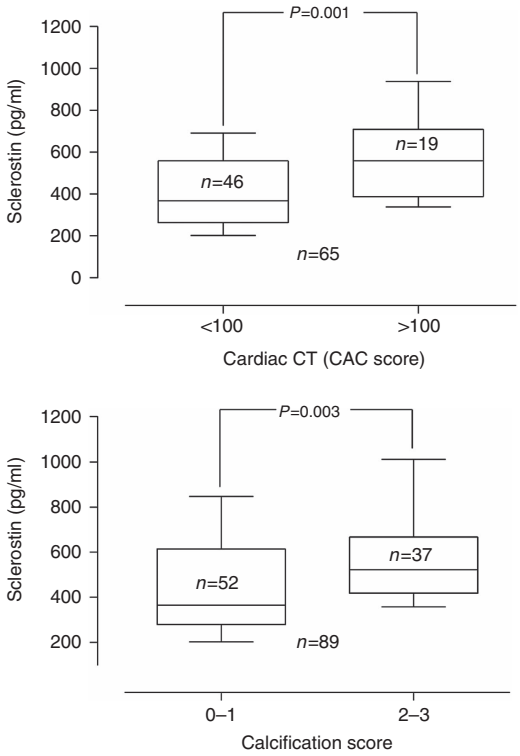

Figure 1 | Sclerostin levels in relation to cardiac computed tomography (CT) score and calcification score. Serum concentrations of sclerostin in 65 patients with Agatston coronary artery calcification (CAC) score (by CT of the heart) of <100 AU vs. >100 AU (top). At the bottom is serum concentrations of sclerostin in 89 end-stage renal disease (ESRD) patients with none or minimal ($n=52$) versus moderate or extensive ($n=37$) histological signs of medial vascular calcification in the epigastric artery.

Table 2 | Multiple regression models of determinants for plasma sclerostin with multiple imputation in end-stage renal disease patients

	Model (β, P) ($r^2=0.32$)
Age (years)	0.41 (**0.001**)
Calcium (mmol/l)	0.04 (0.74)
S-creatinine (μmol/l)	0.30 (**0.01**)
bALP (μg/l)	−0.15 (0.20)
AGE, skin autofluorescence	0.09 (0.48)
iPTH (ng/l)	−0.25 (**0.05**)

Abbreviations: AGE, advanced glycation end products; bALP, bone alkaline phosphatase; iPTH, intact parathyroid hormone. Significant data in bold.

$P=0.006$), male gender (1.82 (1.03–1.16); $P=0.03$) and middle+high sclerostin tertiles versus low sclerostin tertile (3.67 (1.23–11.02); $P=0.02$) were significantly associated with the presence of vascular calcification. After further correction for diabetes, body mass index, TNF, and IGF-1, the association between middle+high tertiles versus low sclerostin tertile and vascular calcification remained significant (2.11 (1.02–4.34); $P=0.04$). Receiver operating characteristics for prediction of vascular calcification (score 2+3) were calculated for sclerostin (area under the curve (AUC) 0.68; $P=0.01$), total CAC score (AUC 0.75; $P=0.0001$; $n=65$), IGF-1 (AUC 0.64; $P=0.04$), and TNF (AUC 0.63; $P=0.02$) (Figure 3). None of the other inflammatory or CKD-MBD biomarkers predicted vascular calcification.

Scoring by semiautomated quantification. A strong correlation ($P<0.001$) was observed between scoring of vascular calcification by the pathologist (AW) and the semiautomated quantification of vascular calcification (Supplementary Figure 1). As expected, median vascular calcification was higher ($P=0.001$) in patients with (8.3%) versus without (1.3%) diabetes mellitus. Moreover, median vascular calcification was more severe ($P<0.001$) in patients with (12.5%) versus without (1.3%) CVD. Males (2.0%) had more marked ($P=0.012$) vascular calcification compared with females (0.8%). In univariate analysis, vascular calcification (%) correlated significantly with age ($\rho=0.57$; $P<0.0001$), hsCRP ($\rho=0.30$; $P=0.004$), TNF ($\rho=0.24$; $P=0.03$), sclerostin ($\rho=0.32$; $P=0.003$), CAC score ($\rho=0.64$; $P<0.001$), advanced glycation end-products autofluoresence ($\rho=0.32$; $P=0.009$), and IGF-1 ($\rho=-0.32$; $P=0.003$). No correlations were observed between vascular calcification (%) and vintage, creatinine, iPTH, ALP, bALP, klotho, FGF23, inactive, active, or total osteocalcin. In a multivariate regression model (Supplementary Table 1) using continuous data, the correlation between log sclerostin with log calcification (%) achieved borderline significance ($P=0.06$) when corrected for age, gender, and diabetes. When log hsCRP was also introduced to the model, the association between log sclerostin and log calcification (%) lost significance ($P=0.08$).

Determinants of CAC

A multivariable GENMOD regression analysis (including age, gender, diabetes, and sclerostin tertiles) showed that diabetes (RR 2.17 (1.12–4.22); $P=0.02$) but not age $\geq$median (RR 2.88 (0.96–8.67); $P=0.05$), male gender (RR 0.83 (0.38–1.81); $P=0.63$), or sclerostin mid+high tertiles versus low tertile (RR 2.10 (0.70–6.31); $P=0.18$) were significantly associated with the presence of CAC score >100 AU in 65 patients.

Vascular *SOST* mRNA expression in relation to phenotype

Arterial expression of *SOST* mRNA was relatively low overall. No correlation was observed between circulating sclerostin levels and vascular *SOST* mRNA expression ($n=55$; ρ 0.01; $P=0.94$). Whereas no differences in median vascular *SOST* mRNA expression were observed between non-diabetes vesus diabetes (7.7 (1.0–30.2) vs. 3.3 (0.3–50.6); $P=0.21$) and patients without vascular calcification versus vascular calcification (8.5 (1.0–31.6) vs. 5.1 (0.4–24.9); $P=0.33$), patients with CVD had lower vascular *SOST* mRNA expression compared with non-CVD patients (2.7 (0.3–13.5) vs. 7.7 (0.9–31.2); $P=0.04$) (Supplementary Figure 2). There were no significant associations between vascular *SOST* mRNA and age ($\rho=0.01$; $P=0.92$), body mass index ($\rho=0.02$; $P=0.89$), gender, hsCRP ($\rho=$ -0.09; $P=0.52$), or CAC score ($\rho=0.16$; $P=0.30$).

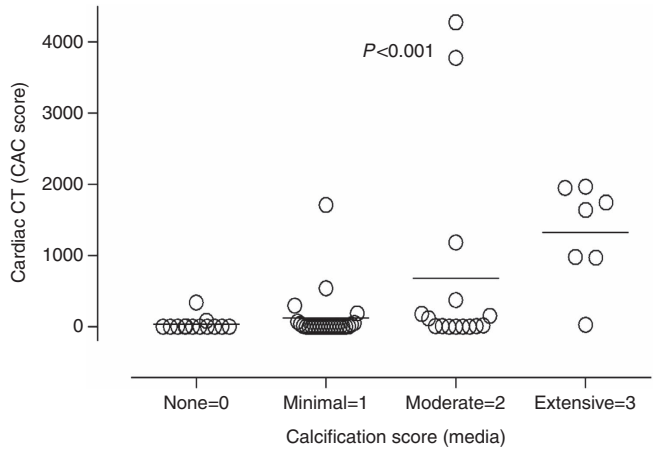

Figure 2 | Relation of coronary artery calcification (CAC) score and calcification score. Total Agatston CAC score by computed tomography (CT) of the heart ($n = 65$) related to the degree of medial vascular calcification (0–3) scored by a pathologist.

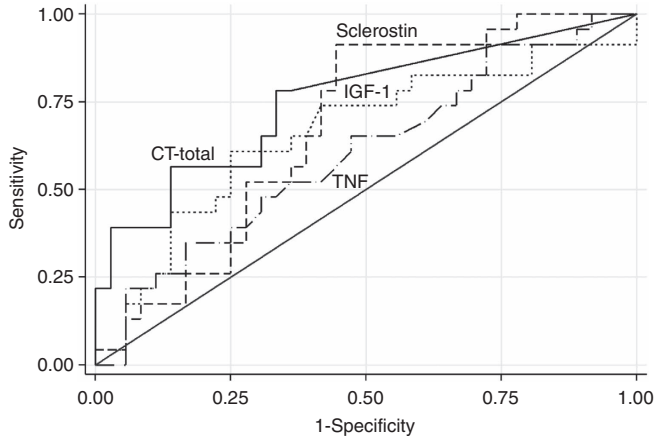

Figure 3 | Receiver operating characteristic (ROC) curves for prediction of vascular calcification. ROCs for prediction of vascular calcification (score 2+3) in the arteria epigastrica by sclerostin (area under the curve (AUC) 0.68; $P = 0.01$), Agatston coronary artery calcification (CAC) score (AUC 0.77; $P = 0.0001$; $n = 65$), insulin growth factor-1 (IGF-1) (AUC 0.64; $P = 0.04$), and tumor necrosis factor (TNF) (AUC 0.63; $P = 0.02$).

Immunohistochemistry

Staining for arterial sclerostin was performed with two different antisclerostin antibodies (Sigma-Aldrich, St Louis, MO and Santa Cruz Biotechnology, Dallas, TX) at various concentrations. However, no distinctly positive staining could be detected, neither in calcified nor in non-calcified specimens (Supplementary Figure 3).

DISCUSSION

Although we investigated a selected group of younger ESRD patients, histological evidence of medial vascular calcification was present in 42% of the patients, confirming premature vascular aging in ESRD.[2,3] The increased cardiovascular risk in the calcified group is mirrored by elevated troponin T. A chief finding of the study is that among a broad range of CKD-MBD biomarkers, only serum sclerostin predicted the presence of vascular calcification in uremic arteries. The positive association between medial vascular calcification and serum sclerostin levels persisted following correction for confounders. We also report that ESRD patients with CAC score >100 AU (Figure 1) and CVD had higher circulating sclerostin levels. It is worth noting that Claes *et al.*[22] reported that the association between sclerostin and aortic calcification (by lumbar X-ray) switched from positive to negative when 'CVD history' was introduced in the multivariate analysis. It could be debated whether or not 'CVD history' should be included in a multivariate model as CVD is an effect of vascular calcification rather than its cause. The difference in GFR between the present cohort and the cohort of CKD 1–5 patients in the study by Claes *et al.*[22] could also explain these divergent findings.

Sclerostin and bALP: interaction between Wnt signaling and promoters of mineralization

In the present study, an inverse correlation was observed between sclerostin and bALP, which confirms previous findings of negative relationships between serum sclerostin and markers of bone formation[15,24] and histomorphometric parameters of bone turnover.[26] Bone-specific ALP is regarded as a better reflector of bone turnover than PTH and is strongly associated with short-term mortality in dialysis patients.[7] Upregulation of ALP and pyrophosphate hydrolysis is increasingly recognized as a potential mechanism of uremic vascular calcification,[27] and serum ALP predicts mortality in ESRD.[28] Even though the increased ALP activity in calcifying vascular smooth muscle cells is exclusive to bALP,[29] it is still unknown to which extent vascular calcification contributes to circulating total ALP or bALP activities. An interaction between Wnt signaling and promoters of mineralization may occur in the process of vascular calcification.[8] Sclerostin inhibits bone formation by inhibition of the Wnt signaling pathway and subsequent downregulation of the transcription factor RUNX2. Although RUNX2 is induced in vascular calcification, reports on the effect of Wnt inhibition in this context are divergent. It is also still unclear whether the effect of Wnt inhibition on vascular calcification is mainly exerted through a direct vascular process or via the induction of an adynamic bone phenotype.

Vascular SOST/sclerostin expression

Didangelos *et al.*[30] were the first to describe sclerostin in human arteries and detected sclerostin in the subintima of non-calcified ascending aortas. A significant upregulation of *SOST* mRNA was reported in calcified aortic valves[20,31] and in calcified skin lesions from patients with calcific uremic arteriolopathy.[32] In addition, animal studies demonstrated increased sclerostin expression in vascular smooth muscle cells and aortas *ex vivo* and *in vivo* in uremia.[33,34] To the best of our knowledge, the colocalization of *SOST* mRNA expression with medial vascular calcification has never previously been assessed in human arteries. In our cohort, vascular *SOST*

mRNA expression was relatively low overall and did not differ between uremic vessels with and without calcification, suggesting that sclerostin in arteries is not a trigger for calcification in smooth muscle cells. This finding contrasts to previous studies of other calcified tissues.[20,31] It can be speculated that diverging results are an effect of using different vascular tissues (aortic valves vs. epigastric arteries), different control populations (i.e. healthy controls vs. ESRD patients with no-minimal vascular calcification), and different analytical methods (analysis of RNA from paraffin-embedded material with risk of RNA degradation vs. material stored in AllProtect, quality controlled with Agilent Bioanalyzer (Agilent Technologies, Santa Clara, CA), and analyzed with specific TaqMan probes). However, we do see significantly lower expression of *SOST* mRNA in ESRD patients with CVD, which might imply a protective effect of upregulation of sclerostin in vessels. Roforth *et al.*[35] reported an inconsistency between increased circulating sclerostin and the expression of sclerostin mRNA in bone, suggesting the contribution of extraosseous sclerostin to serum concentrations. However, as we report no correlation between vascular *SOST* mRNA expression and circulating sclerostin levels, this suggests that vascular-derived sclerostin is not a major contributor to circulating levels. Our negative finding with regard to sclerostin in uremic vessels supports the notion that significant expression of sclerostin does not occur even in heavily calcified vessels. Indeed, most sclerostin is expressed in the nucleus of osteocytes[36]—a cell not expected to be present in arteries. Although our results imply that most of the circulating sclerostin originates from the bone, we do not know if locally produced sclerostin in the bone (and vasculature), which spill over to the systemic circulation, have systemic effects.

Elevated TNF and low IGF-1: promoters of vascular calcification

In obese mice fed a high-fat diet, TNF upregulates the expression of sclerostin through the nuclear factor-κB signaling pathway.[37] Thus, the link between sclerostin and inflammatory conditions, such as ESRD,[38] needs further studies as it could be speculated that this is one pathway by which chronic inflammatory disorders suppress bone formation. However, as no associations were demonstrated between circulating levels of sclerostin and inflammatory biomarkers, inflammation-stimulated expression of sclerostin may not be a major pathway of reduced bone formation in uremia. However, a small but significant difference in TNF levels between ESRD patients with and without vascular calcification suggests a role for TNF in the calcification process.[39] We also found lower IGF-1 levels in the calcified group of patients and a significant negative correlation between IGF-1 and vascular calcification (%). Indeed, IGF-I has a critical position in the maintenance of normal vascular smooth muscle cell phenotype and protection from factors known to stimulate vascular calcification.[40] Thus, further studies are needed to define the permissive role of IGF-1 in the calcification process.

Strengths and limitations

The present study has several strengths and limitations. An obvious strength is the extensive phenotyping and that medial vascular calcification was directly ascertained in arterial biopsies and not evaluated by indirect surrogate markers of vascular calcification, such as aortic calcification by lumbar X-ray,[22] aortic valve calcification by echocardiography,[31] or arterial stiffness by pulse wave analysis.[41] Based on the close correlation between the degree of medial vascular calcification in the epigastric artery and CAC score, we conclude that vascular calcification in the epigastric artery reflects the calcification process in the general arterial tree. Furthermore, medial vascular calcification of the epigastric artery was associated with the presence of clinical CVD. The strong association between calcification scoring by a pathologist and semiautomated quantification of vascular calcification (Supplementary Figure 1 online) also strengthens the study. Limitations of the present study include the rather limited number of patients and the cross-sectional nature of the study, which precludes determination of cause and effect. Moreover, the present results solely rely on epigastric arteries, and, hence, direct comparability to previous studies on *SOST* expression in other parts of the cardiovascular system is not possible. Nevertheless, this is, to the best of our knowledge, the largest clinical material of arterial biopsies collected in ESRD patients. We also acknowledge that the ESRD patients in this study represent a selected group of younger and healthier patients with a more active lifestyle, as they were selected for living donor RTx. Thus, our findings may not be applicable to older, sicker, and sedentary dialysis patients. This selection bias could also explain the lower serum sclerostin concentrations in the current study compared with earlier reports on patients with different stages of CKD, including CKD5D, as a more active lifestyle could lead to decreased serum sclerostin levels through increased mechanical loading.[36] Another potential explanation to the different sclerostin levels could be that different sclerostin enzyme-linked immunosorbent assays (ELISAs) were used. Moreover, although we report a significant association between sclerostin and the presence of vascular calcification, the rather low AUC (0.68) implies that sclerostin is not a useful biomarker to detect vascular calcification in the clinical setting. Population ancestry is associated with different susceptibility for osteoporosis and atherosclerosis.[8] However, as mostly Caucasian patients were included in the present study, race has not affected the results in a major way. Finally, in light of the conflicting results on relations between circulating sclerostin and calcification[20,22] and clinical outcome,[9,23–25] respectively, comparative analyses of different commercial serum sclerostin assays and evaluation of possible protein modifications of sclerostin that may occur in the uremic milieu are warranted.

CONCLUSIONS

High circulating levels of sclerostin in ESRD patients were associated with the degree of vascular calcification ascertained

by histology of arterial biopsies, semiautomated quantification of vascular calcification, and by CAC score. The results of this study suggest that only serum sclerostin (out of a range of several CKD-MBD biomarkers) identifies ESRD patients with vascular calcification. However, the usefulness of sclerostin as a predictor of vascular calcification in the clinical setting appears to be limited. CAC by CT of the heart is a better predictor of the degree of vascular calcification. As vascular expression of *SOST* mRNA and immunohistochemical staining for sclerostin did not associate with circulating levels, or differ between calcified and non-calcified vessels, our data suggest that vascular-derived sclerostin is not a major contributor to circulating sclerostin levels in the uremic milieu.

MATERIALS AND METHODS

Adult ESRD patients undergoing living donor RTx at the Department of Transplantation Surgery at Karolinska University Hospital were invited to participate in the study, which was approved by the regional committee of ethics in Stockholm and adhered to the statutes of the Declaration of Helsinki Principles. Basic characteristics of the 89 included patients are outlined in Table 1. A majority of the patients were Caucasians (however, ethnic background is not registered). Their median age was 46 (range 24–62) years and 63% were males. The causes of ESRD were chronic glomerulonephritis ($n=29$), polycystic kidney disease ($n=18$), diabetes ($n=7$), and other renal diseases, such as Alport's syndrome, interstitial nephritis, nephrosclerosis, amyloidosis, vasculitis, and renal dysplasia ($n=25$), as well as unknown renal disease ($n=10$). The most commonly used forms of medication before RTx were erythropoiesis-stimulating agents ($n=70$), non-calcium-based phosphate binders ($n=66$), angiotensin-converting enzyme inhibitors and/or angiotensin receptor blockers ($n=51$), and loop diuretics ($n=57$). Before RTx, 17 of the patients had previously been diagnosed with cerebrovascular, cardiovascular, and/or peripheral vascular disease (grouped as CVD). Of these patients, two had suffered from cerebrovascular disease (stroke), four had had one or more myocardial infarctions, two had clinical signs of ischemic heart disease (angina pectoris), six had peripheral ischemic atherosclerotic vascular disease, one patient had a history of an aortic aneurysm, one patient had mitral stenosis, and one patient had cardiac failure. Out of the 89 patients, 35 patients (39%) received conservative treatment before undergoing preemptive living donor RTx, whereas 54 patients (61%) underwent dialysis treatment before RTx for a median period of 1.0 (0.2–3.7) years, by hemodialysis ($n=22$, 25%) or by peritoneal dialysis ($n=32$, 36%), or both, as two patients who initially received peritoneal dialysis later on switched to hemodialysis.

Arterial biopsies

Within 20 min after skin incision at the start of surgery, one piece (1–2 cm in length) of the inferior epigastric artery was collected by sharp dissection. Samples were immediately placed in All Protect Tissue Reagent (Qiagen, Hilden, Germany), snap frozen in isopentane, and subsequently stored at −70 °C, or fixed in 4% phosphate-buffered formalin. Formalin-fixed materials from the epigastric arteries were embedded in paraffin. One- to two-µm-thick sections were stained with hematoxylin and eosin and von Kossa staining, respectively. An experienced pathologist (AW) evaluated the sections. The degree of medial calcification (Figure 4) was

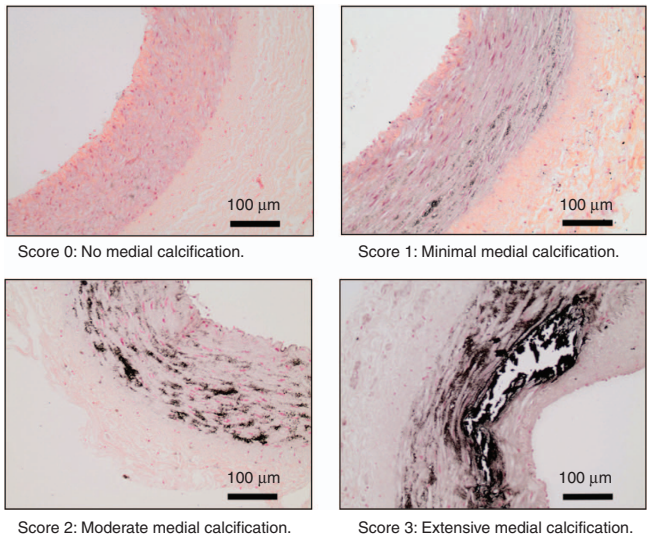

Figure 4 | Histological pictures of the four degrees of medial calcification. Histological pictures (von Kossa staining) representing four categories of the degree of medial vascular calcification in inferior epigastric artery from a total of 89 end-stage renal disease (ESRD) patients in whom biopsies were scored by a pathologist (AW) as having no (score = 0; $n=16$), minimal (score = 1; $n=36$), moderate (score = 2; $n=24$), or extensive (score = 3; $n=13$) signs of medial vascular calcification.

semiquantified on the von Kossa-stained sections and graded 0 to 3, where 0 indicated no calcification and 3 the highest degree of calcification. Patients graded as 0 ($n=16$) and 1 ($n=36$) were combined into group 1 representing no-minimal vascular calcification ($n=52$), and those having moderate (score 2; $n=24$) or extensive (score 3; $n=13$) signs of vascular calcification were combined into group 2 ($n=37$).

Semiautomated quantification of media calcification

To assess the degree of vascular calcification as a continuous variable, we used semiautomated quantification. Briefly, von Kossa-stained slides were captured at four times magnification using a Nikon Eclipse E1000 light microscope (Nikon, Tokyo, Japan). The tunica media and intima of each slide were manually identified and the area was measured using the ImageJ software (http://rsb.info.nih.gov/ij/). Next, a threshold was set to select the calcified area, and the degree of calcification was calculated as calcified area/area of tunica media and intima.

Vascular SOST mRNA expression

Total RNA was prepared from 55 arterial biopsies using TRIzol Reagent (Ambion, Life Technologies, Carlsbad, CA). RNA quantity and quality were determined using a NanoDrop ND-1000 spectrophotometer (NanoDrop products, Wilmington, DE) and Agilent RNA 6000 Nano Assay Kit (Agilent Technologies, Santa Clara, CA), respectively. Random hexamers and SuperScript III (Invitrogen, Life Technologies, Carlsbad, CA) were used for cDNA synthesis. To quantify the relative gene expression of *SOST*, TaqMan gene expression assays for *SOST* were performed and normalized against hypoxanthine phosphoribosyl-transferase 1 (*HPRT1*) and glyceraldehyde-3-phosphate dehydrogenase (*GAPDH*) gene expression using QuantStudio 7 Flex system and Expression Suite Software v 1.0.4 (Applied Biosystems, Life Technologies, Carlsbad, CA).

Immunohistochemistry

Sections from frozen arteries were air-dried and postfixed in 50% ice-cold methanol before immunohistochemical staining using an overnight incubation at 4 °C with rabbit anti-sclerostin antibody (SAB 1300086; Sigma-Aldrich; 1:100 dilution) and the Lab Vision Ultra Vision™ ONE Detection System with HRP Polymer and DAB Plus Chromogen (Thermo Fisher Scientific, Cheshire, UK). Paraffin-embedded arteries (five samples from each calcification group) were cut in 1-μm-thick sections, deparaffinized, rehydrated, and incubated with low pH antigen unmasking solution (Vector Laboratories, Peterborough, UK) in a 2100 retriever (PickCell Laboratories, Amsterdam, The Netherlands). The sections were then immersed in 3% H_2O_2 in methanol, treated with 4% normal serum, and blocked with avidin and biotin (Vector Laboratories). Sections were incubated with a rabbit anti-sclerostin antibody (sc-130258; Santa Cruz; 1:300 dilution) at 4 °C overnight, and then by a biotinylated secondary antibody for 60 min, and finally incubated with a Vector ABC Reagent and developed with a DAB substrate (both Vector Laboratories). Immunohistochemical staining using an overnight incubation at 4 °C with rabbit anti-sclerostin antibody (SAB 1300086; Sigma-Aldrich; 1:100 dilution) also showed no positive staining.

Cardiac CT protocol and analysis

Cardiac CT scans were performed using a 64-channel detector scanner (LightSpeed VCT; General Electric (GE) Healthcare, Milwaukee, WI) in cine mode. Scans were ECG-gated and a standard non-contrast protocol was used with a tube voltage of 100 kV, tube current of 200 mA, 350 ms rotation time, 2.5 mm slice thickness, and displayed field of 25 cm. Calcium deposits in the coronary arteries were identified by a radiologist with Level 2 competence and over 9 years of experience in interpretation of cardiac CT (JR). Data were processed and analyzed using an Advantage Workstation 4.4 (GE Healthcare). Smartscore 4.0 (GE Healthcare) was used to assess CAC scores. Calcified plaques were considered to be present if values crossed the standard threshold of 130 Hounsfield units. CAC scores were expressed in Agatston units (AU) as described previously in detail.[42] Total CAC score was calculated as the sum of the CAC scores in the left main artery, the left anterior descending artery, the left circumflex artery, and the right coronary artery.

Biochemical and other analyses

Sampling was performed the day before RTx. Advanced glycation end-product autofluorescence was measured using an autofluorescence reader (DiagnOptics BV, Groningen, The Netherlands). Dual-energy X-ray absorptiometry ($n = 42$) was performed before Rtx using the DPX-L device (Lunar Corp., Madison, WI) to measure bone mineral density and total fat mass. Analyses of hsCRP, iPTH, plasma cholesterol, triglycerides, HDL-cholesterol, lipoprotein(a), creatinine, albumin, troponin T, calcium, phosphate, magnesium, and D-vitamin were performed with validated routine methods at the accredited Clinical Laboratory of Karolinska University Hospital, Stockholm. Sweden. IGF-1, interleukin-6, and TNF were analyzed by immunometric assays on an Immulite 1000 Analyzer (Siemens Healthcare Diagnostics, Los Angeles, CA) according to the manufacturer's instruction. Similarly, 8-hydroxy-2′-deoxyguanosine was measured using a commercially competitive ELISA Kit (Japan Institute for the Control of Aging, Shizuoka, Japan). Human sclerostin and pentraxin-3 were analyzed with ELISA Kits from R&D Systems (Abingdon, UK). Total osteocalcin (N-MID; IDS, Bolden, UK) as well as inactive (GLU) undercarboxylated osteocalcin (cat. no. MK118) and active (GLA) carboxylated osteocalcin (cat. no. MK111) (Takara Bio, Otsu, Shiga, Japan) were analyzed with Commercial ELISA Kits. Klotho was measured by Human soluble α-Klotho ELISA Assay from IBL International (Hamburg, Germany). Human FGF23 (C terminal) was measured by an ELISA Kit from Immutopics International (San Clemente, CA). Total ALP activity was assessed using a Commercial Reagent Kit (Alkaline Phosphatase (IFCC) Plus; Thermo Fisher Scientific Oy, Vantaa, Finland), and analyzed by an automatic chemical analyzer (Konelab 20XTi; Thermo Electron Corporation, Vantaa, Finland). bALP was measured using the Ostaste BALP ELISA (Immunodiagnostic Systems, Boldon, UK). Fetuin-A was analyzed with ELISA from Epitope Diagnostics (San Diego, CA). Reverse-phase HPLC determined pentosidine in the plasma.[43]

Statistical analyses

Data are expressed as median (range 10th–90th percentile) or percentage or relative RR (95% CI). Statistical significance was set at the level of $P < 0.05$. Comparisons between two groups were assessed with the nonparametric Wilcoxon's test for continuous variables and χ^2 test for nominal variables. Spearman's rank correlation analysis was used to determine associations between selected parameters. We used multivariable GENMOD regression analysis to study the association between the presence of calcification (grades 2 and 3) in the epigastric artery and other parameters. Age (median), gender, diabetes, sclerostin (tertiles), TNF (median), body mass index (median), and IGF-1 (median) were included in the full model. We estimated RR in the GENMOD procedure by introducing a statement (estimate ''Beta' 'variable of interest' $1 - 1/\exp$). We impute laboratory values with SAS procedure called MIANALYZE to avoid excluding patients with missing values. A linear multiple regression model was used to test the continuous data (Supplemenatry Table 1). Receiver operating characteristic curves were plotted and AUCs were calculated. ROC curves were generated by plotting the relationship of the true positivity (sensitivity) and the false positivity (1-specificity) at various cutoff points of the tests, with AUC of 1.0 denoting an ideal test and AUC of 0.5 indicating no diagnostic value. Statistical analyses were performed using statistical software SAS version 9.4 (SAS Campus Drive, Cary, NC).

DISCLOSURE

BL is affiliated with Baxter Healthcare. MS is an employee of Astra Zeneca.

ACKNOWLEDGMENTS

We thank the patients who participated in the study. We are grateful to all those who carried out the extensive clinical and laboratory work (Ann-Christin Bragfors Helin, Björn Anderstam, Monica Eriksson, Sanna Spännare, and Annelie Ring) in the current study. Swedish Medical Research Council (VR) supported PS's and LN's research. Baxter Novum is a result of a grant from Baxter Healthcare to Karolinska Institutet.

SUPPLEMENTARY MATERIAL

Table S1. Multiple regression models of determinants for log % calcification (by semiautomated quantification) in 86 ESRD patients.
Figure S1. Box plots showing association between pathologists scoring of degree of medial vascular calcification (0–3) and semiautomated quantification of degree (%) of vascular calcification by picture analysis.

Figure S2. Box plots showing *SOST* mRNA (RQ) in 55 ESRD patients with (n = 8) and without (n = 47) clinical CVD.
Figure S3. Staining for arterial sclerostin was performed with two different anti-sclerostin antibodies at various concentrations.
Supplementary material is linked to the online version of the paper at http://www.nature.com/ki

REFERENCES

1. Moe S, Drueke T, Cunningham J *et al.* Definition, evaluation and classificationof renal dystrophy; a position statement from Kidney Disease: Improving Global Outcomes (KDIGO). *Kidney Int* 2006; **69**: 1945–1953.
2. Stenvinkel P, Larsson T. Chronic kidney disease: a clinical model of premature aging. *Am J Kidney Dis* 2013; **62**: 339–351.
3. Kooman JP, Kotanko P, AMWJ Schols *et al.* Chronic kidney disease and premature ageing. *Nat Rev Nephrol* 2014; **10**: 732–742.
4. London GM, Guerin AP, Verbeke FH *et al.* Mineral metabolism and arterial functions in end-stage renal disease: potential role of 25-hydroxyvitamin D deficiency. *J Am Soc Nephrol* 2007; **18**: 613–620.
5. Floege J, Kim J, Ireland E *et al.* Serum iPTH, calcium and phosphate, and the risk of mortality in a European haemodialysis population. *Nephrol Dial Transplant* 2011; **2011**: 1948–1955.
6. Gutiérrez OM, Mannstadt M, Isakova T *et al.* Fibroblast growth factor 23 and mortality among patients undergoing hemodialysis. *N Engl J Med* 2008; **359**: 584–592.
7. Drechsler C, Verduijn M, Pilz S *et al.* Bone alkaline phosphatase and mortality in dialysis patients. *Clin J Am Soc Nephrol* 2011; **6**: 1752–1759.
8. Fang Y, Ginsberg C, Seifert M *et al.* CKD-induced wingless/integration1 inhibitors and phosphorus cause the CKD-mineral and bone disorder. *J Am Soc Nephrol* 2014; **25**: 1760–1773.
9. Kanbay M, Siriopol D, Saglam M *et al.* Serum sclerostin and adverse outcomes in non-dialyzed chronic kidney disease patients. *J Clin Endocrinol Metab* 2014; **99**: E1854–E1861.
10. Cejka D, Marculescu R, Kozakowsk iN *et al.* Renal elimination of sclerostin increases with declining kidney function. *J Clin Endocrinol Metab* 2014; **99**: 248–255.
11. Bonani M, Rodriguez D, Fehr T *et al.* Sclerostin blood levels before and after kidney transplantation. *Kidney Blood Press Res* 2014; **39**: 230–239.
12. Sabbagh Y, Graciolli FG, O'Brien S *et al.* Repression of osteocyte Wnt/β-catenin signaling is an early event in the progression of renal osteodystrophy. *J Bone Miner Res* 2012; **27**: 1757–1772.
13. Fang Y, Ginsberg C, Sugatani T *et al.* Early chronic kidney disease-mineral bone disorder stimulates vascular calcification. *Kidney Int* 2014; **85**: 142–150.
14. Register TC, Hruska KA, Divers J *et al.* Sclerostin is positively associated with bone mineral density in men and women and negatively associated with carotid calcified atherosclerotic plaque in men from the African American-Diabetes Heart Study. *J Clin Endocrinol Metab* 2014; **99**: 315–321.
15. Ishimura E, Okuno S, Ichii M *et al.* Relationship between serum sclerostin, bone metabolism markers, and bone mineral density in maintenance hemodialysis patients. *J Clin Endocrinol Metab* 2014; **99**: 4315–4320.
16. Cejka D, Jäger-Lansky A, Kieweg H *et al.* Sclerostin serum levels correlate positively with bone mineral density and microarchitecture in haemodialysis patients. *Nephrol Dial Transplant* 2012; **27**: 226–230.
17. Canalis E. Wnt signalling in osteoporosis: mechanisms and novel therapeutic approaches. *Nat Rev Endocrinol* 2013; **9**: 575–583.
18. McClung MR, Grauer A, Boonen S *et al.* Romosozumab in postmenopausal women with low bone mineral density. *N Engl J Med* 2014; **370**: 412–420.
19. Evenopoel P, D´Haese P, Brandenburg V. Romosozumab in postmenopausal women with osteopenia. *N Engl J Med* 2014; **370**: 1664.
20. Brandenburg VM, Kramann R, Koos R *et al.* Relationship between sclerostin and cardiovascular calcification in hemodialysis patients: a cross-sectional study. *BMC Nephrol* 2013; **14**: 219.
21. Delanaye P, Krzesinski JM, Warling X *et al.* Clinical and biological determinants of sclerostin plasma concentration in hemodialysis patients. *Nephron Clin Pract* 2014; **128**: 127–134.
22. Claes KJ, Viaene L, Heye S *et al.* Sclerostin: another vascular calcification inhibitor? *J Clin Endocrinol Metab* 2013; **98**: 3221–3228.
23. Gonçalves F, Elias RM, Dos Reis LM *et al.* Serum sclerostin is an independent predictor of mortality in hemodialysis patients. *BMC Nephrol* 2014; **15**: 190.
24. Viaene L, Behets GJ, Claes K *et al.* Sclerostin: another bone-related protein related to all-cause mortality in haemodialysis? *Nephrol Dial Transplant* 2013; **28**: 3024–3030.
25. Drechsler C, Evenepoel P, Vervloet MG *et al.* High levels of circulating sclerostin are associated with better cardiovascular survival in incident dialysis patients: results from the NECOSAD study. *Nephrol Dial Transpl* 2014; **30**: 288–293.
26. Cejka D, Herberth J, Branscum AJ *et al.* Sclerostin and Dickkopf-1 in renal osteodystrophy. *Clin J Am Soc Nephrol* 2011; **6**: 877–882.
27. Lomashvili KA, Garg P, Narisawa S *et al.* Upregulation of alkaline phosphatase and pyrophosphate hydrolysis: potential mechanism for uremic vascular calcification. *Kidney Int* 2008; **73**: 1024–1030.
28. Regidor DL, Kovesdy CP, Mehrotra R *et al.* Serum alkaline phosphatase predicts mortality among maintenance hemodialysis patients. *J Am Soc Nephrol* 2008; **19**: 2193–2203.
29. Haarhaus M, Arnqvist HJ, Magnusson P. Calcifying human aortic smooth muscle cells express different bone alkaline phosphatase isoforms, including the novel B1x isoform. *J Vasc Res* 2013; **50**: 167–174.
30. Didangelos A, Yin X, Mandal K *et al.* Proteomics characterization of extracellular space components in the human aorta. *Mol Cell Proteom* 2019; **9**: 2048–2062.
31. Koos R, Brandenburg V, Mahnken AH *et al.* Sclerostin as a potential novel biomarker for aortic valve calcification: an *in vivo* and *ex vivo* study. *J Heart Valve Dis* 2013; **22**: 317–325.
32. Kramann R, Brandenburg VM, Schurgers LJ *et al.* Novel insights into osteogenesis and matrix remodelling associated with calcific uraemic arteriolopathy. *Nephrol Dial Transpl* 2013; **28**: 856–868.
33. Zhu D, Mackenzie NC, Millán JL *et al.* The appearance and modulation of osteocyte marker expression during calcification of vascular smooth muscle cells. *PLoS One* 2011; **6**: e19595.
34. Kramann R, Kunter U, Brandenburg VM *et al.* Osteogenesis of heterotopically transplanted mesenchymal stromal cells in rat models of chronic kidney disease. *J Bone Miner Res* 2013; **28**: 2523–2534.
35. Roforth MM, Fujita K, McGregor UI *et al.* Effects of age on bone mRNA levels of sclerostin and other genes relevant to bone metabolism in humans. *Bone* 2014; **59**: 1–6.
36. Robling AG, Niziolek PJ, Baldridge LA *et al.* Mechanical stimulation of bone *in vivo* reduces osteocyte expression of Sost/sclerostin. *J Biol Chem* 2008; **283**: 5866–5875.
37. Baek K, Hwang HR, Park HJ *et al.* TNF-α upregulates sclerostin expression in obese mice fed a high-fat diet. *J Cell Physiol* 2014; **229**: 640–650.
38. Carrero JJ, Stenvinkel P. Inflammation in end-stage renal disease—what have we learned in 10 years? *Semin Dial* 2010; **23**: 498–509.
39. Tintut Y, Patel J, Parhami F *et al.* Tumor necrosis factor-a promotes *in vitro* calcification of vascular cells via the cAMP pathway. *Circulation* 2000; **102**: 2636–2642.
40. Siddals KW, Allen J, Sinha S *et al.* Apposite insulin-like growth factor (IGF) receptor glycosylation is critical to the maintenance of vascular smooth muscle phenotype in the presence of factors promoting osteogenic differentiation and mineralization. *J Biol Chem* 2011; **286**: 16623–16630.
41. Toussaint ND, Lau KK, Strauss BJ *et al.* Associations between vascular calcification, arterial stiffness and bone mineral density in chronic kidney disease. *Nephrol Dial Transpl* 2008; **23**: 586–593.
42. Agatston AS, Janowitz WR, Hildner FJ *et al.* Quantification of coronary artery calcium using ultrafast computed tomography. *J Am Coll Cardiol* 1990; **15**: 827–832.
43. Suliman ME, Stenvinkel P, Jogestrand T *et al.* Plasma pentosidine and total homocysteine levels in relation to change in common carotid intima-media area in the first year of dialysis therapy. *Clin Nephrol* 2006; **66**: 418–425.